Computational Approach for Understanding the Interactions of UV-Degradable Dendrons with DNA and siRNA

Giovanni M. Pavan,*,† Mauri A. Kostiainen,‡ and Andrea Danani†

Mathematical and Physical Sciences Research Unit (SMF), University for Applied Sciences of Southern Switzerland (SUPSI), Centro Galleria 2, Manno, CH-6928, Switzerland, and Institute for Molecules and Materials, Radboud University Nijmegen, Toernooiveld 1, 6525 ED Nijmegen, The Netherlands

Received: December 2, 2009; Revised Manuscript Received: March 15, 2010

In this work, we present a molecular dynamics study to gain an insight into the binding of nucleic acids with spermine functionalized dendrons. We compare UV-degradable dendrons with nondegradable dendrons studied in our previous works. These two dendritic architectures have the same functional surface; however, the branching scaffold exhibits different flexibilities. Here, we explore how the different branching scaffolds influence the ability to interact with DNA and siRNA. The free energies of binding, calculated with the well-known molecular mechanics Poisson−Boltzmann surface area method, are in good accordance with the experimentally observed binding behavior, demonstrating that the theoretical models are reliable and deliver an accurate description of the systems. In general, the interaction of dendrons with the more flexible siRNA is higher than with rigid double-stranded DNA. Importantly, while binding enthalpy best describes the attraction in general—being in direct relationship with the number of opposite charges interacting in the system—binding entropy is correlated with the distribution of these interactions along the binding interface. Higher uniformity in the binding allows it to maintain a strong enthalpic attraction toward the nucleic acid at lower entropic cost. This entropic cost is due to a loss of degrees of freedom in binding, which is related to the nonuniformity in the energetic contribution of the individual ligands. These findings suggest that the estimation of the pure attraction is not enough to fully understand the binding, but also, information about how this attraction is distributed is needed. This proposes new criteria in the design of DNA and siRNA binding agents.

Introduction

Multivalent ligands that have multiple copies of binding units organized on a single scaffold are important in many biomedical applications.[1] There has been a special interest in using dendritic molecules as scaffolds to organize and manifold binding ligands for the recognition of a wide range of different compounds and especially biomolecules. DNA binding dendrimers have been the focus of active research since the discovery of poly(amidoamine) PAMAM dendrimers.[2−7] Their ability to bind and compact DNA to aid gene transfection has been thoroughly studied.[8−11] DNA binding and packing are among the key features that affect gene transfection. Moreover, understanding the factors that influence the interactions between the DNA and the vector is an important prerequisite for their controlled manipulation. The ionic interaction between a protonated amine and the phosphate backbone of DNA forms the basis for most synthetic DNA binding molecules used for gene delivery. However, an individual binding unit with one protonated amine cannot efficiently bind to the phosphate backbone of DNA under physiological conditions, and to achieve high-affinity binding, multivalent ligands must be utilized.[12−16] This multivalency principle, where the strength of a multivalent binding interaction can be much stronger than the sum of a corresponding number of monovalent interactions, is a common phenomenon throughout nature and has consequently inspired the development in supramolecular chemistry. While the number of binding sites and sizes of the molecules increase, the binding event also becomes more complex to understand and tune. Polyvalent interactions therefore give rise to special phenomena such as cooperativity and multivalency, and the design of such binding systems requires a detailed understanding of the delicate balance between binding entropy and enthalpy.[17−21]

To utilize dendrimers for energetically favorable binding interactions, they should be designed in such a way that the number of binding interactions is maximized while internal strain in the bound molecules is minimized. Both enthalpic and entropic factors must be carefully considered because the enhanced binding energy of multisite attachment must overcome the steric strain induced by the binding event. The high local concentration of binding units and easy structural tunability of dendrimers provide means to investigate how different multivalent ligand architectures influence binding. However, because of the complex nature of multivalent binding that often occurs in the biological environment, experimental insight into the binding is hard to obtain. Computational methods have therefore been used to model multivalent interactions and to gain a deeper insight into the binding mechanism.[22,23]

We have previously synthesized multivalent dendritic ligands with spermine surface groups and Newkome type branching.[12−15,24] These molecules were able to bind DNA with high affinity through multiple electrostatic interactions in a generation-dependent manner. Our recent molecular dynamics modeling of the binding interactions revealed that high affinity binding at a 150 mM NaCl concentration is possible because some ligands sacrifice their binding to partially screen the interaction site from competitor species.[24] However, gene transfection efficiency of these dendrons

* To whom correspondence should be addressed. E-mail: giovanni.pavan@supsi.ch.
† University for Applied Sciences of Southern Switzerland (SUPSI).
‡ Radboud University Nijmegen.

10.1021/jp911439q
Published on Web 04/09/2010

SCHEME 1: Chemical Structure of (a) pllG1 and pllG2 and (b) Spermine Dendrons (G1 and G2)[a]

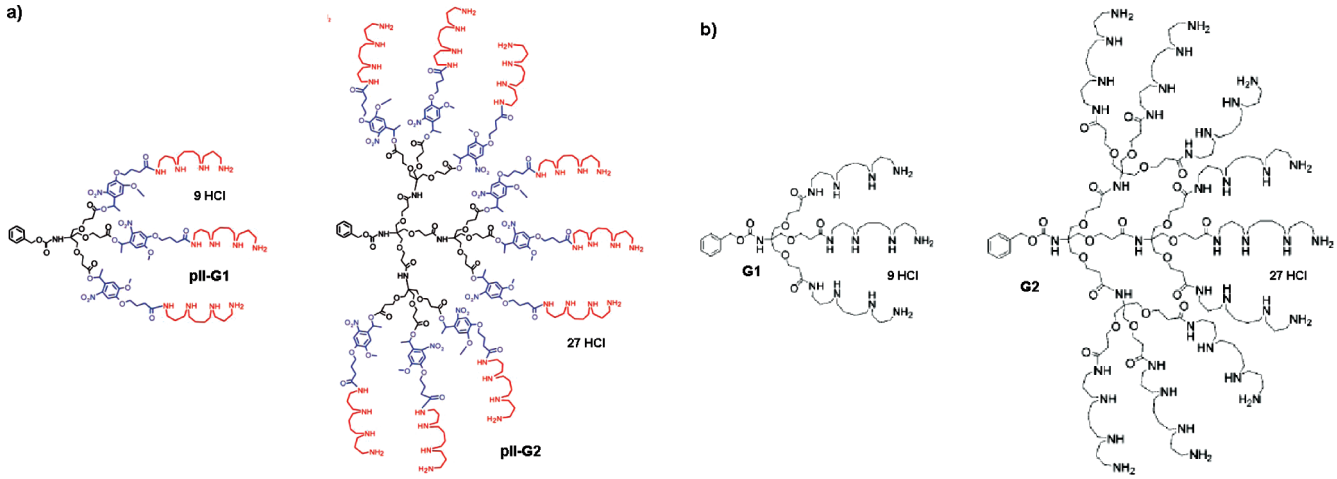

[a] The photolabile linker within pllG1 and pllG2 is represented in blue (a).

remained poor, and consequently, we have developed new dendrons to enhance the DNA delivery and release.[13,25,26] In fact, even the first generation spermine dendrons bind DNA with very high affinity, and consequently, the release is no more possible once the complex is formed. In the last years, many studies focused on dendrimers disassembly[27] and self-immolative dendrimers;[28] the conception of dendritic structures capable of a successful release is a key point in drug delivery. To facilitate the release process, we have prepared UV-degradable dendrons (pllG1 and pllG2, see Scheme 1) that are able to bind DNA with high affinity but can also efficiently release it after a short UV exposure. The affinity of pllG1 and pllG2 toward DNA is slightly higher than our previously reported spermine derivatives of the same generations without the photolabile linker (G1 and G2).[13]

Here, we present a modeling approach to simulate the interactions of pllG1 and pllG2 with DNA and siRNA. Importantly, simulations indicate that the different structures of these dendrons, characterized by higher crowding induced by the photolabile linkers (*o*-nitrobenzyl groups, represented in blue in Scheme 1a), produce higher uniformity in the interactions between each charged amine of the dendrons and the phosphate atoms of DNA and siRNA, reducing the entropic cost and thus enhancing binding. Moreover, we found the siRNA−dendron complex to be more stable than the one with DNA.

Computational Details

All calculations were conducted with the AMBER 10 suite of program.[29] The molecular systems were created according to a previously validated procedure.[23,30] To model the interaction between UV-degradable dendrons and DNA, we used a 21 base pair long B-DNA model containing a mixture of bases (Figure 1a). On the other hand, to model siRNA, we created the GL3 molecule reproducing the correct sequence reported in Figure 1b. Because pllG1 and pllG2 structures are more flexible and smaller in dimensions if compared to the DNA, these models were identified as an ideal compromise between accuracy in reproducing the binding phenomenon and computational time required for simulations.[23,30] Both the 21 base pair double-stranded B-DNA and the GL3 siRNA models were created with the *nucgen* module of AMBER 10. Dendron models (pllG1 and pllG2) were created as composed of three different residues: a central (CEN represented in blue in Figure 2), a repetitive (REP, yellow in Figure 2), and a spermine (SPM, red colored in Figure 2) unit. At neutral pH (∼7.4), each terminal spermine ligand (SPM) was assumed to be charged. In this framework, dendrons pllG1 and pllG2 thus carry +9 and +27 total charges, respectively, located on the amines of spermine surface ligands (each SPM, a +3 charge). The force field types and the partial charges for these residues were obtained using the AM1-BCC[31] calculation method within the *antechamber*[32] module of AMBER 10. This approach has been previously used for the parametrization of dendritic structures[33,30,23] and demonstrated to be particularly accurate in the estimation of free energy calculations.[34] In addition, because *antechamber* assigns parameters and force field types that are consistent with the "general AMBER force field (GAFF)" (*gaff.dat*),[35] the calculated parameters are well-balanced and compatible with the force field parameters of AMBER 10 (details about calculated charges and force field types assigned to atoms of the nonstandard residues are reported in the Supporting Information). Dendron molecules were minimized and equilibrated for 10 ns in NPT conditions explicit solvent to obtain a reliable equilibrated configuration for pllG1 and pllG2. The complexes were created by placing of pllG1 and pllG2 in close proximity of DNA and siRNA major grooves. The consequent four molecular complexes obtained (pllG1 and pllG2 in complex with DNA and siRNA) were again solvated in a periodic box extending 12 Å from the solute containing TIP3P water molecules[36] and the proper amount of Na^+ and Cl^- ions necessary to guarantee the system neutrality and the two relevant salt concentrations of 9.4 and 150 mM NaCl. The counterions were inserted in the water box using the *leap* module of AMBER 10, replacing water molecules where eventual superposition occurred. The final eight systems were initially minimized and then equilibrated (details available in the Supporting Information). The production phase lasted for 10 ns under periodic boundary condition at 300 K and 1 atm, using a time step of 2 fs, the Langevin thermostat, a 10 Å cutoff, the particle mesh Ewald[37] (PME) approach for long-range electrostatic effects, and the SHAKE algorithm.[38] All of the production molecular dynamics were carried out by using the *pmemd* module and the *parm99* all-atom force field by Cornell et al.,[39] working in parallel on 128 processors of the Cray XT5

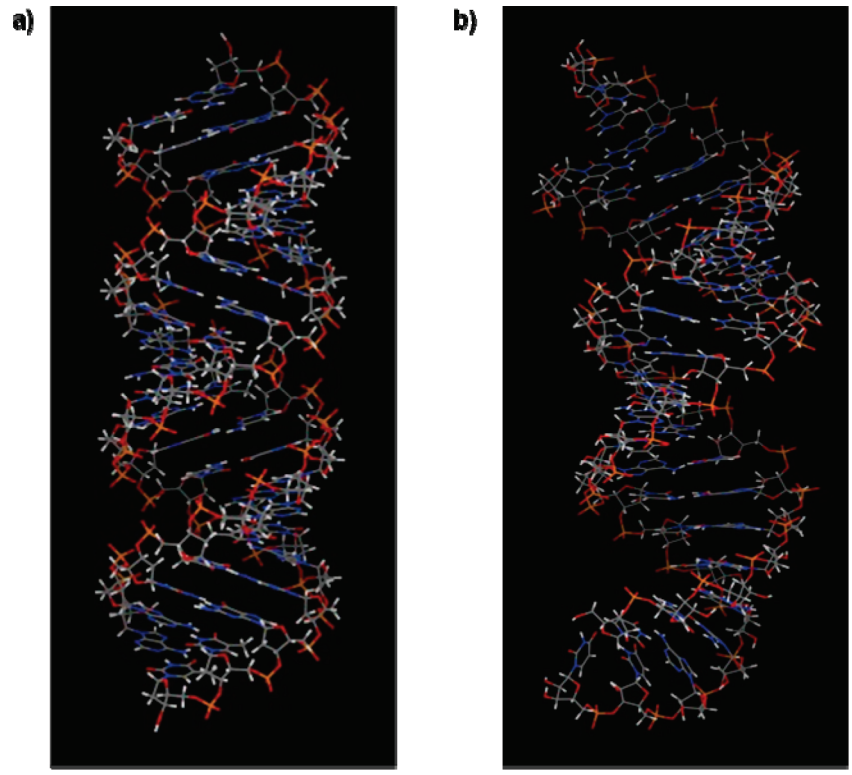

Figure 1. Structures of (a) double helical DNA and (b) GL3 siRNA used for simulations. (a) Antisense: 5′-TCG AAG TAC TCA GCG TAA GTT-3′; sense: 3′-AGC TTC ATG AGT CGC ATT CAA-5′. (b) Antisense: 5′-UCG AAG UAC UCA GCG UAA G dTdT-3′; sense: 3′-dTdT AGC UUC AUG AGU CGC AUU C-5′.

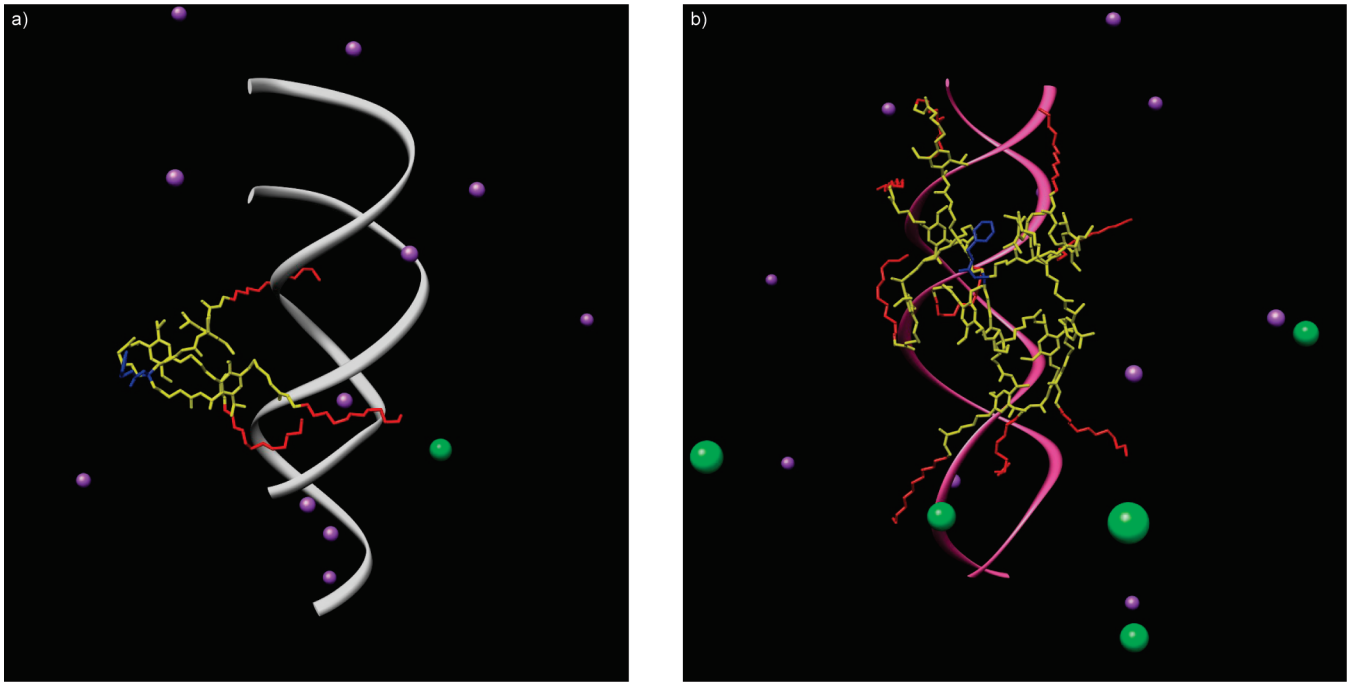

Figure 2. Snapshots of pllG1−siRNA complex at 9.4 mM NaCl concentration (a) and of pllG2−DNA complex at 150 mM NaCl concentration (b). The CEN residue is represented in blue, REP residues are represented in yellow, and SPM charged residues are represented in red. DNA and siRNA are represented as pink and gray solid ribbons, respectively. Only those ions in close proximity of the binding site are present in the pictures. Cl^- ions are colored in green, and Na^+ ions are in purple; water molecules and hydrogen atoms are removed from the image for clarity.

at CSCS Swiss National Supercomputer Center of Manno (Switzerland).

Binding affinities (ΔG_{bind}) were obtained from molecular dynamic simulations and calculated over 200 of snapshots taken from the equilibrated phase of the dynamic trajectories (last 2 ns of the simulation, the interval between each snapshot is 10 ps) using the well-known molecular mechanics Poisson−Boltzmann (PB) surface area (MM-PBSA) approach.[40] ΔG_{bind} is composed by an enthalpic (ΔH_{bind}) and an entropic ($-T\Delta S_{bind}$) term as given in eq 1:

$$\Delta G_{\text{bind}} = \Delta H_{\text{bind}} - T\Delta S_{\text{bind}} \quad (1)$$

$$\Delta H_{\text{bind}} = \Delta E_{\text{gas}} - \Delta G_{\text{sol}} \quad (2)$$

ΔH_{bind} can be further split into total gas phase in vacuo nonbond energy (ΔE_{gas}), composed by an electrostatic and a van der Waals term (ΔE_{ele} and ΔE_{vdW}), and a solvation energy ($\Delta G_{\text{solv}} = \Delta G_{\text{PB}} + \Delta G_{\text{NP}}$)[41] as described in eq 2. The polar component of ΔG_{solv} was evaluated using the PB[42] approach with a numerical solver implemented in the *pbsa* program of AMBER 10.[43] The nonpolar contribution to the solvation energy was calculated as $\Delta G_{\text{NP}} = \gamma$ (SASA) $+ \beta$, in which $\gamma = 0.00542$ kcal/Å^2, $\beta = 0.92$ kcal/mol, and SASA is the solvent-accessible surface estimated with the MSMS program.[44] Finally, the normal-mode[45] approach was used to compute the entropic components. Per residue decomposition energies were obtained using the *mm_pbsa.pl* script available in AMBER 10. Finally, the equilibrated trajectories were processed with the *ptraj* module to obtain structural information, that is, the radius of gyration (R_g) and the radial distribution functions (RDF) (full details about the computational procedures are available in the Supporting Information).

Results and Discussion

In our previous experimental work, the DNA binding and release properties of the dendrons were studied with an ethidium bromide (EthBr) displacement assay.[12,13] This assay utilizes the competition between the DNA binding ligands and the EthBr for binding to DNA. EthBr exhibits intense fluorescence when bound to DNA; however, when it is displaced from the DNA by a DNA binding ligand, its fluorescence is quenched. Binding values are best described by CE_{50} values, which indicate the nominal dendron charge excess (CE) causing a 50% decrease in fluorescence intensity—the lower the CE_{50} is, the stronger the binding. CE is defined here as the nominal "number of positive charges" of the polyamine divided by the "number of negative charges" present on the DNA.

TABLE 1: Previously Reported Experimental Data for the Binding of pllG1, pllG2, and G2 to Calf Thymus DNA as Determined by EthBr Displacement Assay[a]

	CE_{50}[b]	
compound	9.4 mM NaCl	150 mM NaCl
pllG1	0.52 ± 0.021	0.96 ± 0.067
pllG2	0.44 ± 0.045	0.66 ± 0.045
G2	0.81 ± 0.032	0.76 ± 0.040

[a] Higher CE_{50} values represent less effective binding of the dendrons to DNA. [b] CE_{50} represents the charge excess (N:P ratio) required to decrease EthBr fluorescence by 50%.

We studied the binding at two different salt concentrations (9.4 and 150 mM NaCl). Under low-salt conditions (9.4 mM NaCl), the dendritic systems pllG1 and pllG2 bind DNA very strongly with similar strength ($CE_{50} = 0.5$ and 0.4, respectively, Table 1). At high salt concentration (150 mM NaCl), pllG1 and pllG2 are only little affected by the increase of competitive Na^+ ions, due to the multivalent nature of these dendritic systems. The larger pllG2 binds slightly stronger than pllG1 ($CE_{50} =$ 0.7 and 1.0, respectively, Table 1). These CE_{50} values are in good accordance with, although slightly lower than, our previously reported values for spermine derivatives (G2 reported for comparison) without photolabile linker (Table 1).

In this study, the binding with siRNA and DNA was modeled in 150 and 9.4 mM NaCl salt solutions, to reproduce the same conditions as in the experimental study (results reported in Table 1). As mentioned in the Computational Details, the final molecular systems used in the simulations were composed of a single UV-degradable dendron in complex with a single DNA or siRNA molecule. These molecules were immersed in a periodic water box containing a suitable number of Na^+ and Cl^- ions necessary to guarantee the system neutrality and to reproduce the correct ionic strength of the solution as described previously.

All of the calculated free energies of binding, enthalpies, and entropies were normalized over the number of total charged amines (N) to allow comparison between different dendron generations. Table 2 reports the per amine normalized energies expressed in kcal mol^{-1}.

By comparing the differences in the thermodynamic results at the two different salt concentrations, we were able to understand the effect of the ionic concentration on the binding. The complexation of pllG1 and pllG2 with DNA and siRNA is characterized by a strong favorable enthalpic attraction, almost completely driven by the electrostatic interaction of N and P atoms of SPM and DNA/siRNA, respectively, and by an unfavorable entropic term. As evidenced in our previous studies, there is a direct relationship between enthalpy and entropy—the higher the attraction is, the greater the number of degrees of freedom lost during the binding. Importantly, the best binder (in terms of strength of binding) is the one that is able to use actively its surface ligands to bind successfully to the negative charges of the target at the lowest entropic cost. Data in Table 2 show a generation-dependent behavior at 150 mM NaCl. This is, as demonstrated in previous studies,[23] a result of the disturbing actions of couterions present in the system. Na^+ and Cl^- atoms in solution (as will be described in details further) interfere with the SPM ligands that are most exposed to the

TABLE 2: Thermodynamic Parameters Determined by Molecular Dynamics Methods for the Binding of Dendrons to DNA and siRNA[a]

	150 mM			9.4 mM		
system (NaCl)[b]	$\Delta H_{\text{bind}}/N$	$-T\Delta S_{\text{bind}}/N$	$\Delta G_{\text{bind}}/N$	$\Delta H_{\text{bind}}/N$	$-T\Delta S_{\text{bind}}/N$	$\Delta G_{\text{bind}}/N$
pllG1−DNA	−11.1 ± 0.8	+6.5 ± 0.5	−4.6 ± 0.4	−14.7 ± 0.6	+7.0 ± 0.5	−7.7 ± 0.5
pllG1−siRNA	−13.0 ± 0.9	+6.4 ± 0.5	−6.5 ± 0.4	−14.4 ± 0.8	+5.4 ± 0.3	−9.0 ± 0.5
pllG2−DNA	−11.3 ± 0.4	+3.7 ± 0.2	−7.7 ± 0.5	−12.0 ± 0.8	+4.1 ± 0.2	−7.9 ± 0.5
pllG2−siRNA	−11.7 ± 0.3	+3.8 ± 0.2	−7.9 ± 0.4	−13.2 ± 0.7	+4.2 ± 0.2	−9.0 ± 0.6
G2−DNA[b]	−11.5 ± 0.4	+4.2 ± 0.1	−7.3 ± 0.4	−11.5 ± 0.6	+4.2 ± 0.2	−7.3 ± 0.4

[a] Energies are reported for all of the systems at both salt concentrations (150 and 9.4 mM). $\Delta H_{\text{bind}}/N$, $-T\Delta S_{\text{bind}}/N$, and $\Delta G_{\text{bind}}/N$ are the total enthalpic, entropic, and free energies of binding (ΔH_{bind}, $-T\Delta S_{\text{bind}}$, and ΔG_{bind}) normalized per charged amine to allow energetic comparison between different generations. All per amine energies are expressed in kcal mol^{-1}. [b] Energetic values for G2−DNA complex at 150 and 9.4 mM NaCl were calculated in our previous work.[23]

TABLE 3: Radius of Gyration (R_g) for Complexes, DNA and siRNA, Dendrons, and SPM Surface Ligands at 150 mM NaCl[a]

system (150 mM)[b]	complex	nucleic acid	dendron	SPM
pllG1 + DNA	20.9 ± 1.2	21.7 ± 1.1	11.1 ± 0.5	13.5 ± 0.5
pllG1 + siRNA	19.4 ± 0.9	19.6 ± 0.8	12.8 ± 0.6	16.6 ± 0.6
pllG2 + DNA	20.8 ± 1.0	21.2 ± 0.9	16.2 ± 0.8	20.1 ± 0.9
pllG2 + siRNA	20.0 ± 1.1	20.9 ± 0.9	15.2 ± 0.6	18.8 ± 0.7
G2 + DNA	20.4 ± 1.1	21.7 ± 1.1	15.4 ± 0.7	18.1 ± 0.8

[a] R_g values are reported in angstroms. [b] R_g values for systems in 9.4 mM NaCl conditions are available in the Supporting Information.

surrounding solution during the binding process and decrease their binding efficacy. However, while pllG2 has enough surface ligands to compensate this loss of efficiency and maintain the same binding efficacy, pllG1 has not. In fact, pllG2 is able to screen the surrounding ions with the external surface ligands, which allows the inner spermines to bind stronger to the DNA. That is why at 150 mM NaCl the charged amines of pllG1 lose binding efficiency if compared with the ones of pllG2 (Table 2: from 1.4 to 3.1 kcal mol^{-1} of decrease in siRNA and DNA $\Delta G_{bind}/N$, respectively, with a 95% confidence interval for these estimates of 1.1 and 1.3, respectively).

The observed loss in binding affinity is completely due to a higher entropic cost. The binding enthalpy strictly follows the number of charges, and thus, the enthalpic attraction of each N charged atom ($\Delta H_{bind}/N$) can be considered constant. On the other hand, the entropic advantage of pllG2 when compared to pllG1 is evident—the difference in the entropic cost is 2.8 kcal mol^{-1} (with a 95% confidence interval of 1.1) in DNA binding and 2.6 kcal mol^{-1} (with a 95% confidence interval of 1.1) in siRNA binding. This demonstrates that three pllG1 molecules at the same time (+27 total dendrons charge) bind DNA and siRNA with lower affinity than one single pllG2 molecule (charge +27)—clear evidence of multivalency.

At low salt concentration (9.4 mM NaCl), both pllG1 and pllG2 bind DNA and siRNA in similar manner. Generally, UV-degradable dendrons bind stronger to siRNA than to DNA. This is largely due to the higher flexibility of GL3 molecule when compared to DNA and is a consequence of a higher uniformity in the structure and vibrations of the complexes. Surprisingly, even if pllG2 is supposed to be more rigid than G2, data in Table 2 indicate that pllG2 exhibits the same enthalpic attraction when compared to G2 despite a lower entropic cost. This interesting result can be explained by a higher uniformity in the binding site induced by the steric crowding of the photolabile linkers and will be further discussed in detail.

Geometrical and structural analyses were performed to gain a different point of view into the binding behavior. Table 3 reports the radius of gyration (R_g) for the dendron−DNA/siRNA complexes, nucleic acids, dendrons, and the surface ligands (SPM), all in the presence of 150 mM NaCl (see the Supporting Information for R_g values at 9.4 mM NaCl). R_g is not a true radius but is defined as the root-mean-square distance between each atom and the center of mass of a given molecule. R_g gives important information on the geometrical structure of these systems. R_g values for SPM ligands are bigger than the ones for the whole dendrons, because the core atoms are not taken in account. In general, increasing the salt concentration of the solution increases the dimensions of the dendron and SPM because external ions attract the spermine ligands and thus stretch the dendrons. An exception of this is the pllG1−DNA complex that shows higher R_g values at 9.4 mM NaCl (Supporting Information: 11.3 and 15.6 Å for dendron and SPM, respectively). This difference is consistent with the reduced binding affinity of pllG1 toward DNA at 150 mM NaCl that is due to the disturbing actions of Na^+ and Cl^- atoms and to the high rigidity of DNA strands (Table 2: $\Delta G_{bind}/N$ changes from −6.5 in siRNA binding to −4.6 kcal mol^{-1}, while binding DNA—a difference of 1.9 kcal mol^{-1} with a 95% confidence interval of 1.1).

Interesting insight into the ability of the ligands to adapt to the binding target can be obtained by comparing the R_g values between SPM and dendron. The bigger this difference is, the higher the orientation. It is evident that, to maintain a high binding efficiency toward DNA, pllG1 at 9.4 mM NaCl needs to stretch its branches (SPM−dendron difference in R_g is 4.3 Å at 9.4 mM NaCl vs 2.4 Å at 150 mM NaCl). On the contrary, the more flexible siRNA is able to adapt to the small pllG1 surface better, reducing the entropic cost of binding from +7.0 to +5.4 kcal mol^{-1}—the variation is 1.6 kcal mol^{-1} with a 95% confidence interval of 1.2). However, even though the DNA binding affinity is somewhat reduced, it remains considerably high as is evident from the high enthalpic values in Table 2.

To have a more exhaustive interpretation of the binding event, we performed an analysis on RDF of the atoms that are most actively participating to the binding. RDF represents the density and the distribution of atoms in space with respect to the center of mass of the dendron. Because RDF is calculated at each step of the simulation, it gives information on the position occupied by a certain atom at a certain time. These profiles are obtained as an average over all of the simulations steps and thus give indication about the spatial density as well as about the ability of each atom of the dendron to move in the space during the binding. Therefore, high and narrow peaks in a small area of these graphs mean not only high density of atoms in a certain zone but also high localization and low mobility of these atoms. On the other hand, broad and low intensity peaks indicate low density of atoms with high vibrations. For this analysis, we focused on pllG2−DNA and pllG2−siRNA complexes at 150 mM NaCl and we compared the RDF profiles with those of G2−DNA complex. Figure 3 reports RDF profiles for positive charged atoms of SPM residues (N, colored in blue) and negatively charged atoms of DNA and siRNA (P, pink). Figure 3a,b reports the results for pllG2−DNA and pllG2−siRNA complexes, respectively. RDF for G2−DNA complex is reported to compare the different dynamic behavior driven by the steric crowding induced by *o*-nitrobenzyl groups in the branches. RDF profiles for the dendrons and nucleic acids at 150 mM NaCl concentration are available in the Supporting Information.

The main difference in binding behavior of pllG2 and G2 is represented in Figure 3. In the case of G2, high blue and pink peaks can be observed (Figure 3c); however, the high peaks are absent in the case of pllG2 (Figure 3a,b). This difference identifies a low mobility area in the binding site of G2−DNA complex. Interestingly, the central spermines of G2 have a higher flexibility, which allows a deeper penetration into the DNA double helix. This results in a nonuniform binding, which is focused into the central part of the binding site and characterized by N and P atoms that are almost fixed at the distance of 5−10 Å. On the other hand, the rigid core of pllG2 induces a different behavior—it maintains the dendrons structure more ordered. The

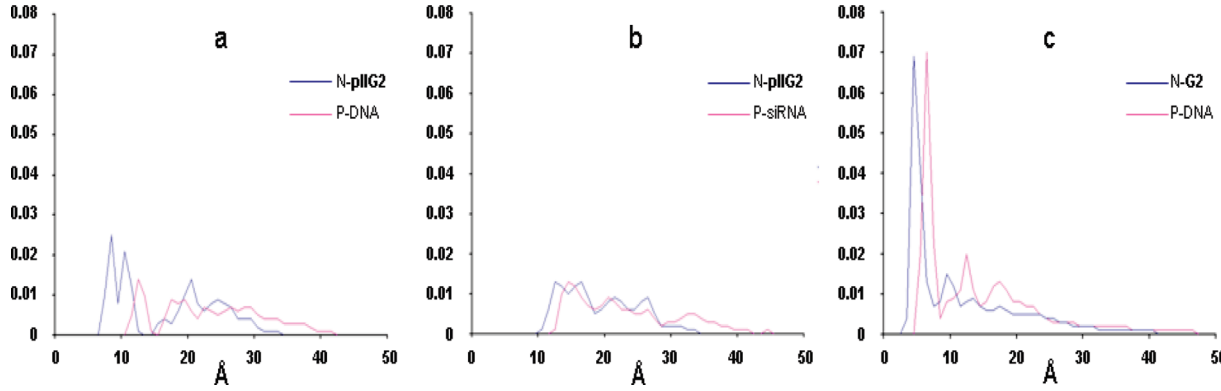

Figure 3. RDF for charged amines (N, blue) and for P atoms (pink). (a) pllG2−DNA complex, (b) pllG2−siRNA complex, and (c) G2−DNA complex. RDF profiles were obtained at a 150 mM NaCl concentration. Distances from the dendrons center of mass are expressed in angstroms.

TABLE 4: Interaction Energies (E_{tot}) Determined for Individual SPM Residues on the Dendron Interacting with DNA and siRNA at 150 mM NaCl[a]

SPM[b]	pllG2−DNA	pllG2−siRNA	G2−DNA[c]
1	−22.0 ± 3.9	−25.9 ± 5.6	−18.3 ± 1.7
2	−17.8 ± 2.1	−22.4 ± 2.0	−29.4 ± 3.5
3	−8.4 ± 0.8	−8.2 ± 0.5	−28.9 ± 2.9
4	−35.4 ± 2.4	−30.1 ± 1.4	−36.1 ± 5.5
5	−20.7 ± 3.0	−7.7 ± 0.4	−23.6 ± 2.5
6	−21.4 ± 1.5	−19.8 ± 3.3	−9.5 ± 0.4
7	−24.2 ± 2.7	−23.5 ± 2.2	−18.1 ± 3.4
8	−24.9 ± 2.2	−34.5 ± 3.0	−9.7 ± 1.5
9	−11.9 ± 3.3	−6.1 ± 0.4	−18.4 ± 2.1
mean E_{tot} ± SD[d]	−23.8 ± 5.6	−26.0 ± 5.4	−24.7 ± 7.0

[a] E_{tot} represents the total in vacuo energy after the correction for solvation. All E_{tot} values are reported in kcal mol^{-1}. [b] Interaction energies E_{tot} are reported for SPM residues only (identified by numbers in Figure 4). [c] E_{tot} values for the G2−DNA complex were calculated in our previous work.[23] [d] Mean E_{tot} values and related standard deviations (SDs) are calculated over the SPMs that actively participate to the binding (E_{tot} < −15 kcal mol^{-1}). SD values reflect the uniformity of binding.

surface ligands are thus better distributed in the binding site, and the charged amines are able to move coherently with P atoms of DNA and siRNA. The strength and stability of the binding are represented here by the high superposition of blue and pink curves (Figure 3a,b), indicating that N and P charged atoms are vibrating together at each simulation step with the same frequency.

The higher binding uniformity of pllG2 produces the same enthalpic attraction when compared to G2 (∼−11.4 kcal mol^{-1} in average), although at a lower entropic cost (+3.7 vs +4.2 kcal mol^{-1}—a decrease of 0.5 kcal mol^{-1} with a 95% confidence interval of 0.4). The more unfavorable entropic value is due to the loss of degrees of freedom in the less mobile zone of the binding site (high peaks in Figure 3c).

To support these observations in a quantitative way, we performed a per residue decomposition of the receptor/ligand interaction energy, which can quantify the affinity of each residue of the dendron (CEN, REP, and SPM) to the nucleic acid. Our previous study on spermine dendrons[23,30] demonstrated that the binding phenomena of the electrostatic interactions between N positive and P negative charged atoms are orders of magnitude higher than the total contribution given by CEN and REP residues. All of the binding affinity is consequently focused on the surface SPM ligands. For clarity, Table 4 reports therefore only contributions of SPM units to binding for the three systems of interest. Each single SPM ligand is identified by a numerical index as shown in Figure 4.

The energetic components reported in Table 4 can be defined in terms of eq 3. These values represent the difference between the energy of the molecular complex ($E_{complex}$) and the sum of the energies of dendron and DNA/siRNA taken separately ($E_{dendron} + E_{DNA}$). Negative energy values indicate attractive forces and the thermodynamic tendency to form a complex.

$$E = E_{complex} - (E_{dendron} + E_{DNA}) \quad (3)$$

Gas-phase energies (E_{gas}) for each residue are composed of electrostatic and van der Waals interaction contributions (E_{ele} and E_{vdw}, respectively) according to eq 4.

$$E_{gas} = E_{ele} + E_{vdW} \quad (4)$$

The in vacuo gas-phase energy for each residue (E_{gas}) is then corrected for solvation to give the total energy E_{tot}. The *mm_pbsa.pl* script of AMBER 10 does not support the PB solvation method for residue energy decomposition; therefore, the generalized Born (GB) method was used to correct the gas-phase energies for solvation. Energy decomposition for nonpolar contributions to desolvation is performed using the LCPO method.[46] However, the trends from the two approaches are in excellent agreement, and this deconvolution approach is particularly useful as it allows us to determine the relative binding effects of each individual residue. It is evident how pllG2 can bind DNA more uniformly than G2 (Figure 4). It is worth noting that the overall binding uniformity of spermine dendrons is much higher when compared to other rigid dendritic carriers (for example, high generation PAMAM dendrimers). Figure 4 shows that not all of the surface ligands are actively involved in the binding at high salt concentration. A small number of SPM units "sacrifice" their interaction with DNA and siRNA (identified by individual E_{tot} contribution less favorable than −15 kcal mol^{-1} in Table 4) and act as an "umbrella", screening the binding site from the disturbing action of counterions. These residues are SPM 3 and SPM 9 in pllG2−DNA complex; SPM 3, SPM 5, and SPM 9 in pllG2−siRNA complex; and SPM 6 and SPM 8 in G2−DNA complex, respectively. These surface ligands are characterized by less favorable E_{tot} values as seen in Table 4 and by less efficient binding interactions as shown in Figure 4. This behavior is consistent with our previous work on spermine dendrons.[23]

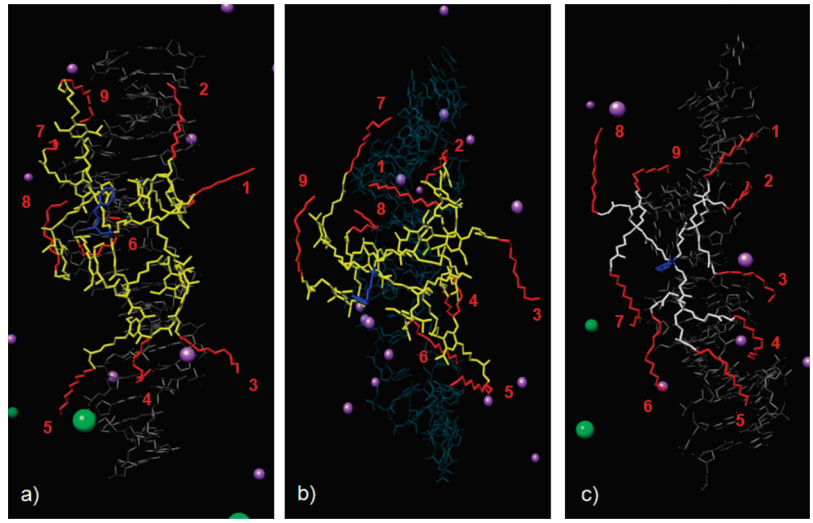

Figure 4. Snapshots of the molecular dynamics simulation of pllG2−nucleic acid complex (a), pllG2−siRNA complex (b), and G2−DNA complex (c) in the presence of 150 mM NaCl. Dendron CEN is shown in blue, REP is shown in yellow, and light gray is used for pllG2 and G2, respectively. The SPM ligands are shown and numbered in red. The DNA and GL3 siRNA are portrayed in shadowed dark and cyan, respectively. Water molecules and hydrogen atoms are omitted for clarity, and only those counterions in close proximity to the complexes are shown.

The last row of Table 4 reports the average E_{tot} value (mean) and the corresponding standard deviation (SD) of all the SPM residues that are actively participating to the binding ($E_{tot} < -15$ kcal mol^{-1}). The screening residues, which do not take part in active binding, are excluded from these calculations. E_{tot} mean values for pllG2−DNA and G2−DNA complexes are on the same range (statistically equivalent), indicating that both pllG2 and G2 attract DNA with each charged amine in a similar way (in average). The same is true for pllG2 binding siRNA. It is interesting to compare the SD of E_{tot} mean value between different complexes. SD values for pllG2 are similar for both siRNA and DNA binding but approximately 25−30% lower than for G2. We find this result to be very important and in agreement with all of the observations presented here. Higher SD in E_{tot} values can be explained by higher nonuniformity in the spreading of the total interaction energy on all of the surface ligands. In G2−DNA complex, the binding strength is focused on the central residues: SPM 2, SPM 3, SPM 4, and SPM 5. This is consistent with the nonuniformity in vibrations as observed in the RDF profiles. Furthermore, it is also the explanation for the higher entropic cost required by G2 to achieve the same enthalpic affinity as pllG2 in DNA binding.

Conclusions

In this work, we have presented molecular dynamic methods to study the binding of UV-degradable dendrons to DNA and siRNA at different salt concentrations. We were able to reproduce the same trends observed in the experimental DNA binding studies, indicating that the molecular models used in this study are reliable. We used different data analysis techniques to gain a unique insight into the experimentally observed high DNA binding affinity values. Importantly, we found out that the entropy of the binding system can explain the observed variations, suggesting that they originate from structural differences between pllG2 and G2. In particular, the crowding of the branches, induced by the photolabile linker, results in a rigid structure that is able to support the spermine ligands.

By decomposing the total receptor/ligand interaction energy for each binding ligand, we were able to point the attention on those spermines that actively participate to the binding. Furthermore, we investigated how, and why, pllG2 is able to maintain the same enthalpic affinity toward DNA when compared to G2 with a reduced entropic cost. The pllG2 dendron is able to use its surface ligands more uniformly, avoiding preferential binding spots into the binding site. This results in a uniform vibrational behavior of N and P charged atoms that belong to dendron and DNA and thus in a stable binding. Finally, higher affinity toward siRNA was demonstrated and explained by the higher curvature and flexibility of the GL3 molecule.

Concluding, in these electrostatic-driven phenomena, there is an intuitive analogy between enthalpy and interacting charges and between entropic cost and degrees of freedom sacrificed in the binding. This study points out that the distribution in space of a certain attraction and the entity of the attraction itself are equally important and indivisible factors. This provides new hints into the definition of flexibility properties and moves the attention from binding strength to binding efficiency, suggesting new paradigms in the design of molecules devoted to interact with nucleic acids.

Acknowledgment. We acknowledge the COST action TD0802, "Dendrimers in Biomedical Applications", in favoring this collaborative program of research. G.M.P. and A.D. also acknowledge the CSCS Swiss National Supercomputer Center of Manno (Switzerland) for their support and for the generous access to the 22128 cores of the new Cray XT5-Rosa supercomputer. M.A.K. acknowledges support from the Academy of Finland, Instrumentarium Science Foundation, and the Alfred Kordelin Foundation.

Supporting Information Available: Detailed information about the molecular systems simulated in this work, calculated free energies of binding, radii of gyration, and RDF plots for dendrons in complex with DNA and siRNA at both of the relevant salt concentrations (150 and 9.4 mM NaCl). This material is available free of charge via the Internet at http://pubs.acs.org.

References and Notes

(1) Mammen, M.; Choi, S.-K.; Whitesides, G. M. *Angew. Chem., Int. Ed.* **1998**, *37*, 2754–2794.

(2) Jiang, D.-L.; Aida, T. *Prog. Polym. Sci.* **2005**, *30*, 403–422.
(3) Fréchet, J. M. J. *Proc. Natl. Acad. Sci. U.S.A.* **2002**, *99*, 4782–4787.
(4) Smith, D. K.; Hirst, A. R.; Love, C. S.; Hardy, J. G.; Brignell, S. V.; Huang, B. *Prog. Polym. Sci.* **2005**, *30*, 220–293.
(5) Lee, C. C.; MacKay, J. A.; Frechet, J. M. J.; Szoka, F. C. *Nat. Biotechnol.* **2005**, *23*, 1517–1526.
(6) Gillies, E. R.; Frechet, J. M. J. *Drug Discovery Today* **2005**, *10*, 35–43.
(7) Cloninger, M. J. *Curr. Opin. Chem. Biol.* **2002**, *6*, 742–748.
(8) Boas, U.; Heegaard, P. M. H. *Chem. Soc. Rev.* **2004**, *33*, 43–63.
(9) Haensler, J.; Szoka, F. C. *Bioconjugate Chem.* **1993**, *4*, 372–379.
(10) Kukowska-Latallo, J. F.; Bielinska, A. U.; Johnson, J.; Spindler, R.; Tomalia, D. A.; Baker, J. R. *Proc. Natl. Acad. Sci. U.S.A.* **1996**, 93.
(11) Tang, M. X.; Redemann, C. T.; Szoka, F. C., Jr. *Bioconjugate Chem.* **1996**, *7*, 703–714.
(12) Kostiainen, M. A.; Hardy, J. G.; Smith, D. K. *Angew. Chem., Int. Ed.* **2005**, *44*, 2556–2559.
(13) Kostiainen, M. A.; Smith, D. K.; Ikkala, O. *Angew. Chem., Int. Ed.* **2007**, *46*, 7600–7604.
(14) Kostiainen, M. A.; Szilvay, G. R.; Lehtinen, J.; Smith, D. K.; Linder, M. B.; Urtti, A.; Ikkala, O. *ACS Nano* **2007**, *1*, 103–113.
(15) Kostiainen, M. A.; Szilvay, G. R.; Smith, D. K.; Linder, M. B.; Ikkala, O. *Angew. Chem., Int. Ed.* **2006**, *45*, 3538–3542.
(16) Mulder, A.; Huskens, J.; Reinhoudt, D. N. *Org. Biomol. Chem.* **2004**, *2*, 3409–3424.
(17) Ercolani, G. *J. Am. Chem. Soc.* **2003**, *125*, 16097–16103.
(18) Gestwicki, J. E.; Cairo, C. W.; Strong, L. E.; Oetjen, K. A.; Kiessling, L. L. *J. Am. Chem. Soc.* **2002**, *124*, 14922–14933.
(19) Kitov, P. I.; Bundle, D. R. *J. Am. Chem. Soc.* **2003**, *125*, 16271–16284.
(20) Kitov, P. I.; Sadowska, J. M.; Mulvey, G.; Armstrong, G. D.; Ling, H.; Pannu, N. S.; Read, R. J.; Bundle, D. R. *Nature* **2000**, *403*, 669–672.
(21) Schoen, A.; Freire, E. *Biochemistry* **1989**, *28*, 5019–5024.
(22) (a) Feuerstein, B. G.; Pattabiraman, N.; Marton, L. J. *Nucleic Acids Res.* **1989**, *17*, 6883–3892. (b) Feuerstein, B. G.; Pattabiraman, N.; Marton, L. J. *Nucleic Acids Res.* **1990**, *18*, 1271–1282. (c) Haworth, I. S.; Rodger, A.; Richards, W. G. *Proc. Roy. Soc. B* **1991**, *244*, 107–116. (d) Lyubartsev, A. P.; Nordenskiöld, L. *J. Phys. Chem. B* **1997**, *101*, 4335–4342. (e) Rouzina, I.; Bloomfield, V. A. *Biophys. J.* **1998**, *74*, 3152–3164. (f) Dias, R. S.; Pais, A. A. C. C.; Miguel, M. G.; Lindman, B. *J. Chem. Phys.* **2003**, *119*, 8150–8157. (g) Real, A. N.; Greenall, R. J. *J. Biomol. Struct. Dyn.* **2003**, *21*, 469–487. (h) Deserno, M.; Arnold, A.; Holm, C. *Macromolecules* **2003**, *36*, 249–259. (i) Teif, V. B. *Biophys. J.* **2005**, *89*, 2574–2587. (j) Saito, T.; Iwaki, T.; Yoshikawa, K. *Europhys. Lett.* **2005**, *71*, 304–310. (k) Pastre, D.; Pietrement, O.; Landousy, F.; Hamon, L.; Sorel, I.; David, M. O.; Delain, E.; Zozime, A.; Le Cam, E. *Eur. Biophys. J. Biophys. Lett.* **2006**, *35*, 214–223. (l) Sanchez-Cauasco, S.; Delcros, J. G.; Moya-Garcia, A. A.; Sanchez-Jimenez, F.; Ramirez, F. J. *Biophys. Chem.* **2008**, *133*, 54–65. (m) Dai, L.; Mu, Y. G.; Nordenskiöld, L.; van der Maarel, J. R. C. *Phys. Rev. Lett.* **2008**, *100*, 118301.
(23) Pavan, G. M.; Danani, A.; Pricl, S.; Smith, D. K. *J. Am. Chem. Soc.* **2009**, *131* (28), 9686–9694.
(24) Hardy, J. G.; Kostiainen, M. A.; Smith, D. K.; Gabrielson, N. P.; Pack, D. W. *Bioconjugate Chem.* **2006**, *17*, 172–178.
(25) Kostiainen, M. A.; Rosilo, H. *Chem.—Eur. J.* **2009**, *15*, 5656–5660.
(26) Welsh, D. J.; Jones, S. P.; Smith, D. K. *Angew. Chem., Int. Ed.* **2009**, *48*, 4047–4051.
(27) (a) McGrath, D. V. *Mol. Pharm.* **2005**, *2*, 253–263. (b) Szalai, M. L.; Kevwitch, R. M.; McGrath, D. V. *J. Am. Chem. Soc.* **2003**, *125*, 15688–15689.
(28) (a) Amir, R. J.; Pessah, N.; Shamis, M.; Shabat, D. *Angew. Chem., Int. Ed.* **2003**, *42*, 4494–4499. (b) Weinstain, R.; Sagi, A.; Karton, N.; Shabat, D. *Chem.—Eur. J.* **2008**, *14*, 6857–6861. (c) Sagi, A.; Weinstain, R.; Kanton, N.; Shabat, D. *J. Am. Chem. Soc.* **2008**, *130*, 5434–5435.
(29) Case, D. A.; Darden, T. A.; Cheatham, T. E., et al. *AMBER 10*; University of California: San Francisco, CA, 2008.
(30) (a) Pavan, G. M.; Mintzer, M. A.; Merkel, O. M.; Kissel, T.; Simanek, E. E.; Danani, A. *Biomacromolecules* **2010**, *11*, 721–730. (b) Pavan, G. M.; Albertazzi, L.; Danani, A. *J. Phys. Chem. B* **2010**, *114*, 2667–2675. (c) Jones, S. P.; Pavan, G. M.; Danani, A.; Pricl, S.; Smith, D. K. *Chem. Eur. J.* **2010**, DOI: 10.1002/chem.200902546.
(31) (a) Jakalian, A.; Bush, B. L.; Jack, D. B.; Bayly, C. I. *J. Comput. Chem.* **2000**, *21*, 132–146. (b) Jakalian, A.; Jack, D. B.; Bayly, C. I. *J. Comput. Chem.* **2002**, *25*, 1623–1641.
(32) Wang, J.; Wang, W.; Kollman, P. A.; Case, D. A. *J. Mol. Graphics Modell.* **2006**, *25*, 247–260.
(33) (a) Opitz, A. W.; Wagner, N. J. *J. Polym. Sci., Part B: Polym. Phys.* **2006**, *44*, 3062–3077. (b) Amirkhanov, N. V.; Dimitrov, I.; Opitz, A. W.; Zhang, K.; Lackey, J. P.; Cardi, C. A.; Lai, S.; Wagner, N. J.; Thakur, M. L.; Wickstrom, E. *Bioplymers* **2008**, *89* (12), 1061–1076.
(34) Mobley, D. L.; Dumont, E.; Chodera, J. D.; Dill, K. A. *J. Phys. Chem. B* **2007**, *111*, 2242–2254.
(35) Wang, J.; Wolf, R. M.; Caldwell, J. W.; Kollman, P. A.; Case, D. A. *J. Comput. Chem.* **2004**, *25*, 1157–1174.
(36) Jorgensen, W. L.; Chandrasekhar, J.; Madura, J. D.; Impey, R. W.; Klein, M. L. *J. Chem. Phys.* **1983**, *79*, 926–935.
(37) Darden, T.; York, D.; Pedersen, L. *J. Chem. Phys.* **1998**, *98*, 10089–10092.
(38) (a) Ryckaert, J.-P.; Ciccotti, G.; Berendsen, H. J. C. *J. Comput. Phys.* **1977**, *23*, 327. (b) Krautler, V.; van Gunsteren, W. F.; Hanenberger, P. H. *J. Comput. Chem.* **2001**, *5*, 501.
(39) Cornell, W. D.; Cieplak, P.; Bayly, C. I.; Gould, I. R.; Merz, K. M.; Ferguson, D. M.; Spellmeyer, D. C.; Fox, T.; Caldwell, J. W.; Kollman, P. A. *J. Am. Chem. Soc.* **1995**, *117*, 5179–5197.
(40) Srinivasan, J.; Cheatham, T. E.; Cieplak, P.; Kollman, P. A.; Case, D. A. *J. Am. Chem. Soc.* **1998**, *120*, 9401–9409.
(41) Andricioaei, I.; Karplus, M. *J. Chem. Phys.* **2001**, *115*, 6289–6292.
(42) Jayaram, B.; Sprous, D.; Beveridge, D. L. *J. Phys. Chem.* **1998**, *102*, 9571–9576.
(43) Luo, R.; David, L.; Gilson, M. K. *J. Comput. Chem.* **2002**, *23*, 1244–1253.
(44) Sitkoff, D.; Sharp, K. A.; Honig, B. *J. Phys. Chem.* **1994**, *98*, 1978–1988.
(45) Sanner, M. F.; Olson, A. J.; Spehner, J. C. *Biopolymers.* **1996**, *38*, 305–320.
(46) Weiser, J.; Shenkin, P. S.; Clark Still, W. *J. Comput. Chem.* **1999**, *20*, 217–230.

JP911439Q